Viscoelastic jet formation with impulsive boundary motion using Basilisk

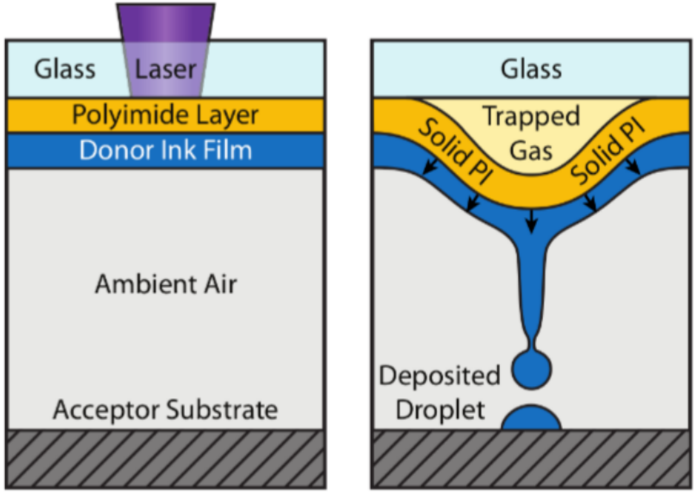

J. Fluid Mech. (2012), vol. 709, pp. 341–370

Emre Turkoz, Luc Deike, Craig B. Arnold
with Jens Eggers
November 16th, 2017
Princeton,NJ

Need of Printing Viscoelastic Materials

Flexible electronics

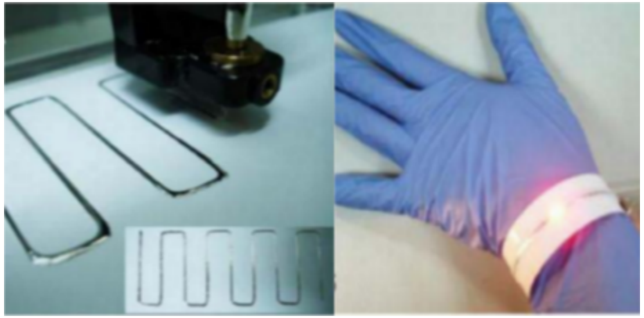

Dababneh, J. Manuf. Sci. Eng 136(6), 061016 (2014)

Sensors

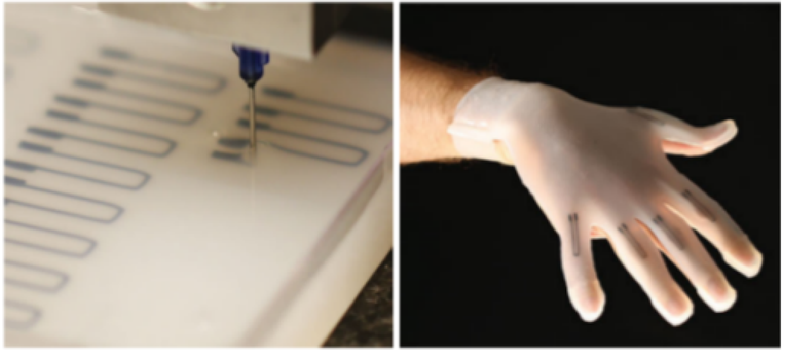

Muth, Adv. Mater. 26, 6307-6312 (2014)

3D printing

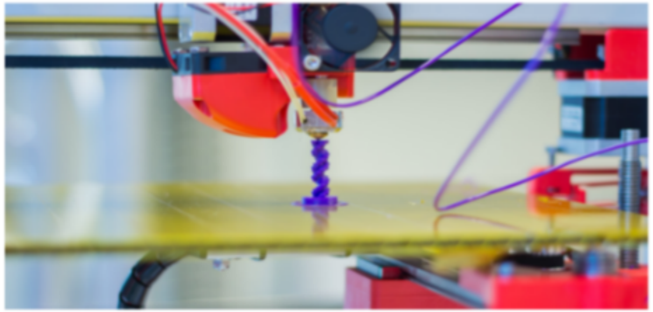

Azimi, Environ. Sci. Technol 50, 1260-1268 (2016)

Tissue engineering

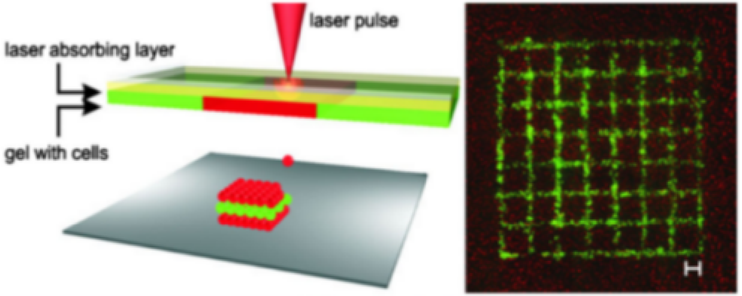

Koch, Biotech. Bioeng. 109.7 (2012)

Printing Techniques

Inkjet printing

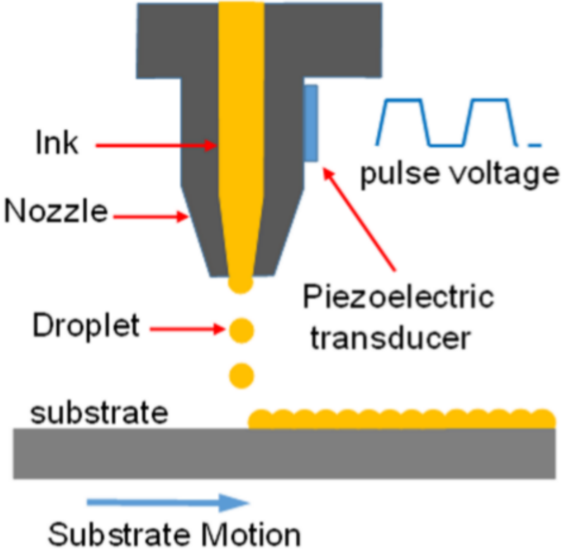

- Nozzle should be designed for the ink and application
- Clogging
- Drop diameters ≥ 10 μm

Laser-induced forward transfer

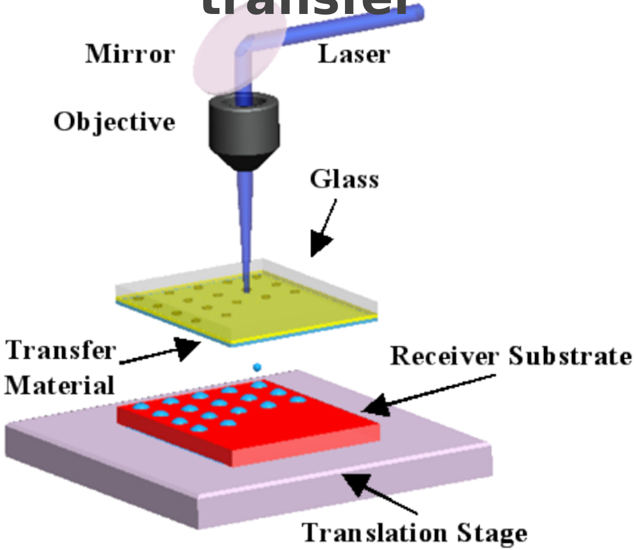

- No nozzle → no clogging
- Droplets with smaller diameters

Blister-Actuated Laser-Induced Forward Transfer (BA-LIFT)

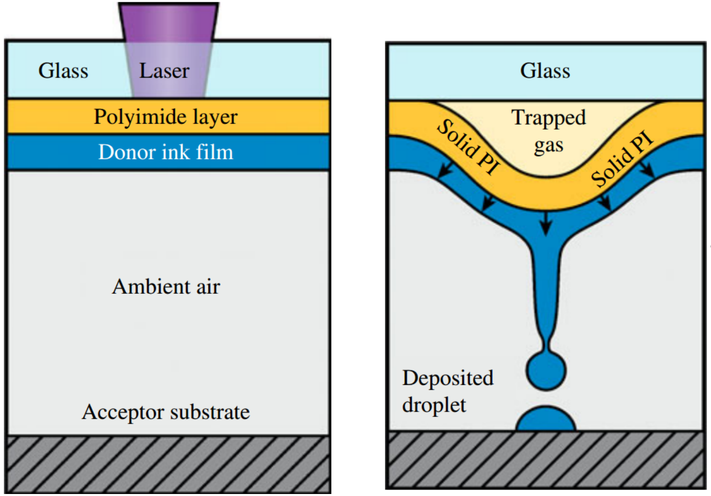

J. Fluid Mech. (2012), vol. 709, pp. 341–370

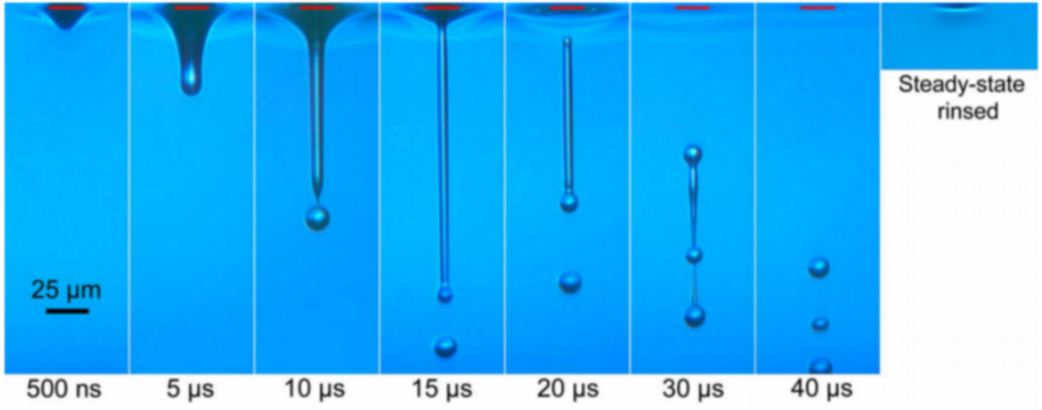

Microfluid. Nanofluid. 11.2, 199-207 (2011)

Mechanical impulse and subsequent jet formation → Droplet pinch-off through Rayleigh-Plateau instability → Material transfer onto acceptor surface

Parameter Space

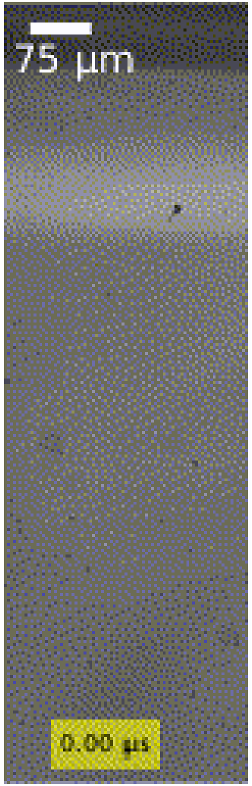

NMP - A newtonian solvent

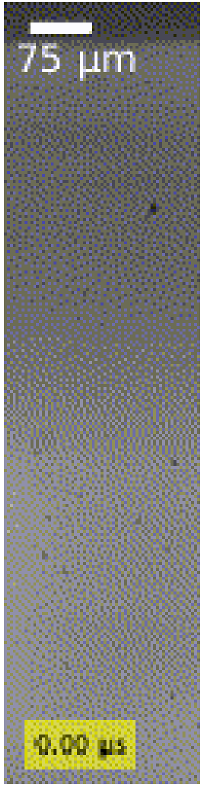

0.1 wt.% xanthan gum in water - A viscoelastic solution

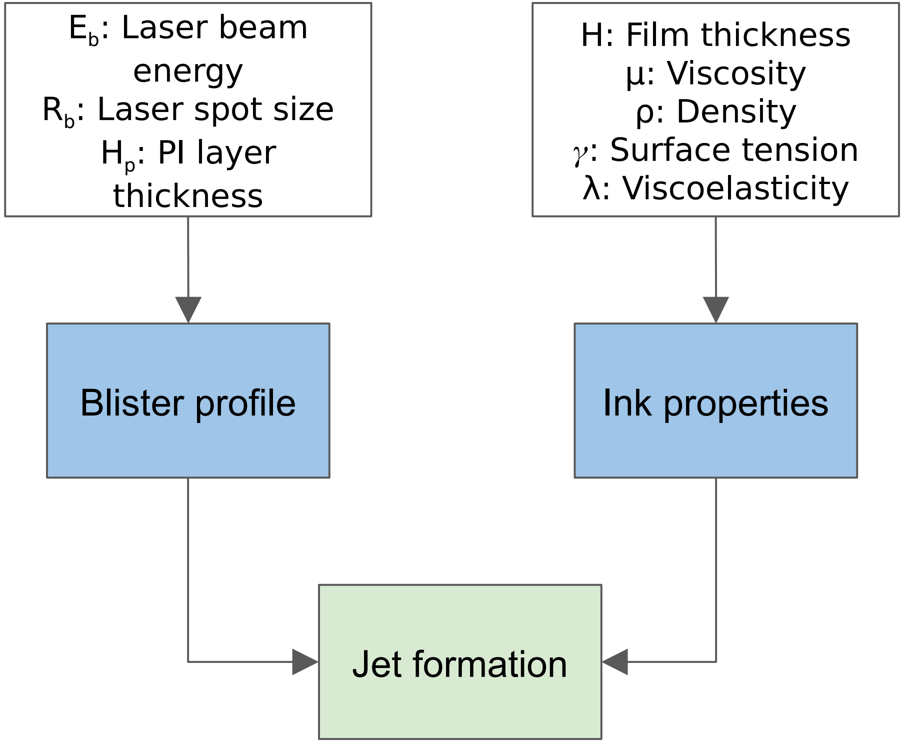

This parameter space determines the outcome of the process

Problem Statement

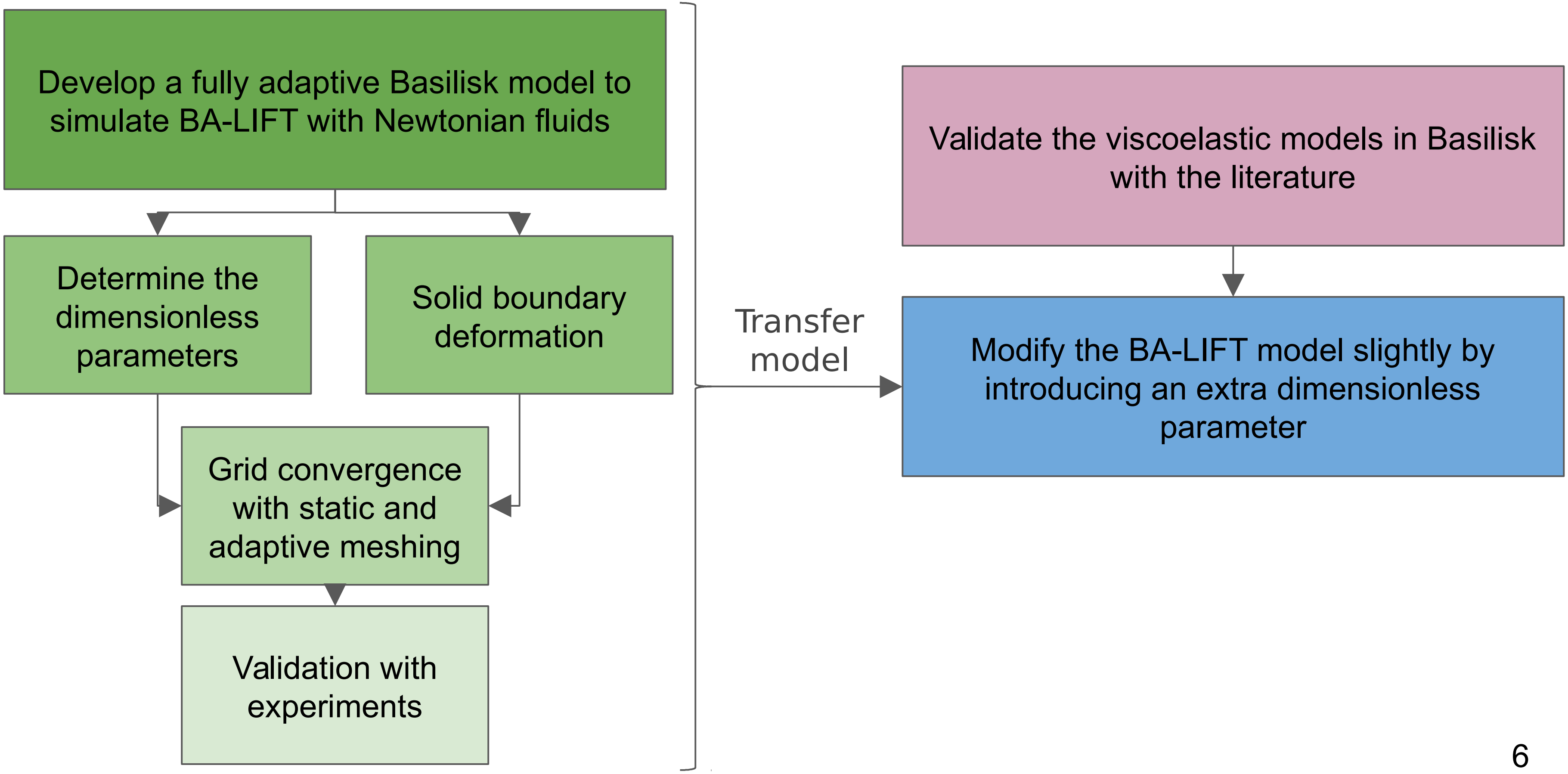

Problem Setup

Three phases
- Polymer
- Ink
- Air

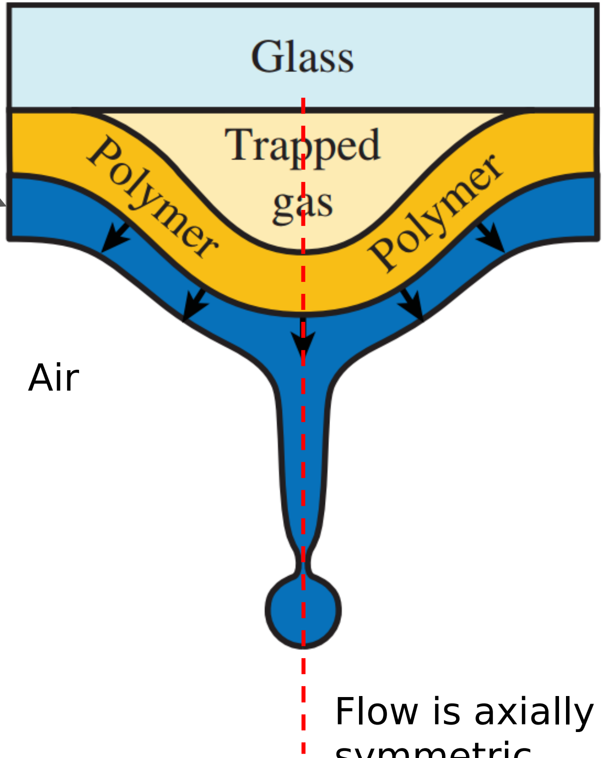

Solid boundary deformation: From empirical measurements [1]

Air

Flow is axially symmetric

[1] J. Fluid Mech. (2012), vol. 709, pp. 341–370

Impulsive Boundary Deformation

- **Boundary deformation during BA-LIFT is already formulated [1]**

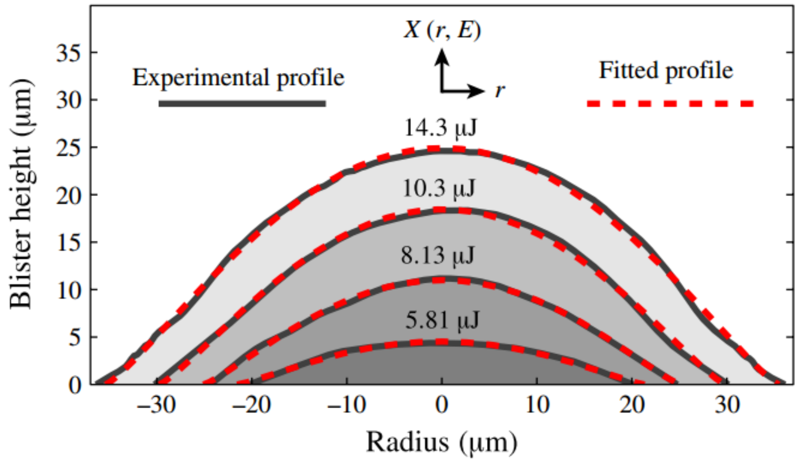

Empirical profile fits for blister profiles

$$\delta(r,E,t) = X(r,E)\cdot T(t)$$

$$X(r,E) = H_0(E)\left(1-\left(\frac{r}{R_0(E)}\right)^2\right)^C$$

$$T(t) = \frac{2}{\pi}\arctan(t/\tau_b)$$

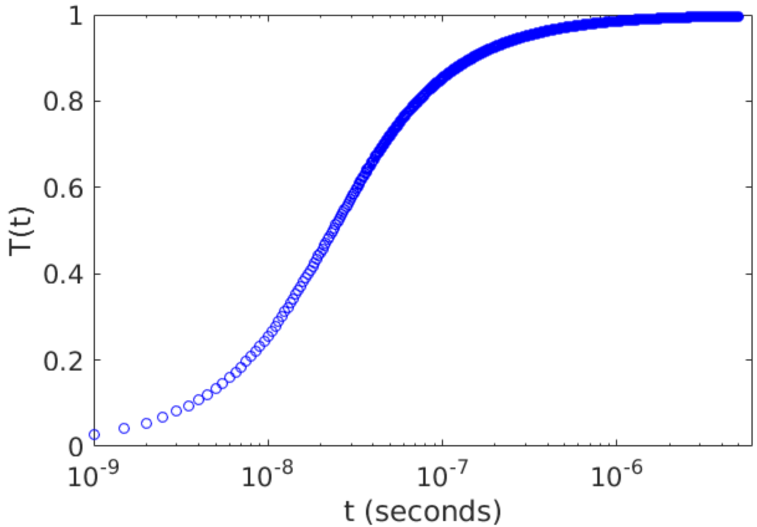

[1] Brown, M. S., Brasz, C. F., Ventikos, Y., & Arnold, C. B. (2012). Impulsively actuated jets from thin liquid films for high-resolution printing applications. Journal of Fluid Mechanics, 709, 341-370.

Non-dimensionalization of the Problem

Experimental parameters

μ_a	Air viscosity
μ_l	Liquid viscosity
ρ_a	Air density
ρ_l	Liquid density
γ	Surface tension
τ_b	Blister expansion time
R_b	Blister radius

Dimensionless numbers

μ_a / μ_l

ρ_a / ρ_l

τ_b / τ_c → Blister expansion time / capillary time scale

$$\mathrm{Oh} = \mu_l / \sqrt{\rho \gamma R_b}$$

$$\tau_c = \sqrt{\rho R_b^3 / \gamma}$$

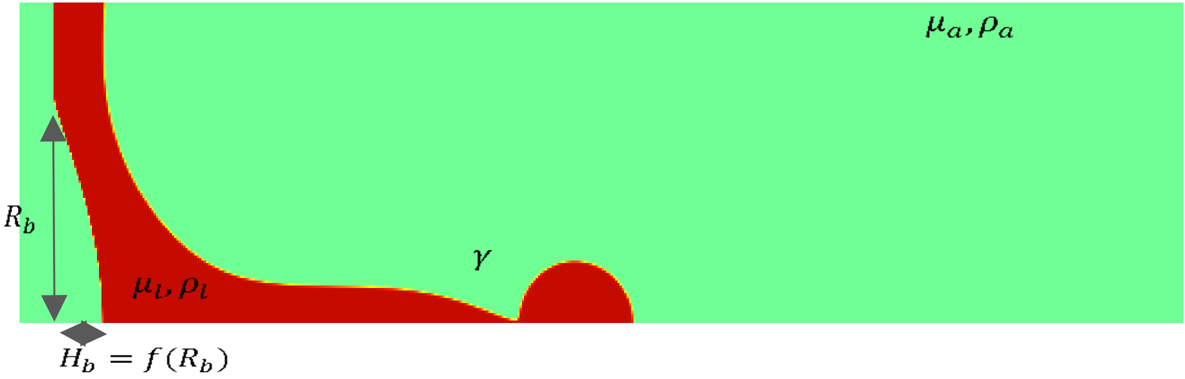

Modeling the solid layer [1,2,3] & Algorithm

- **Solid layer is represented with a tracer (f12)**
- **Reinitialized every time step**
- **Velocity values throughout the solid are assigned at each time step**

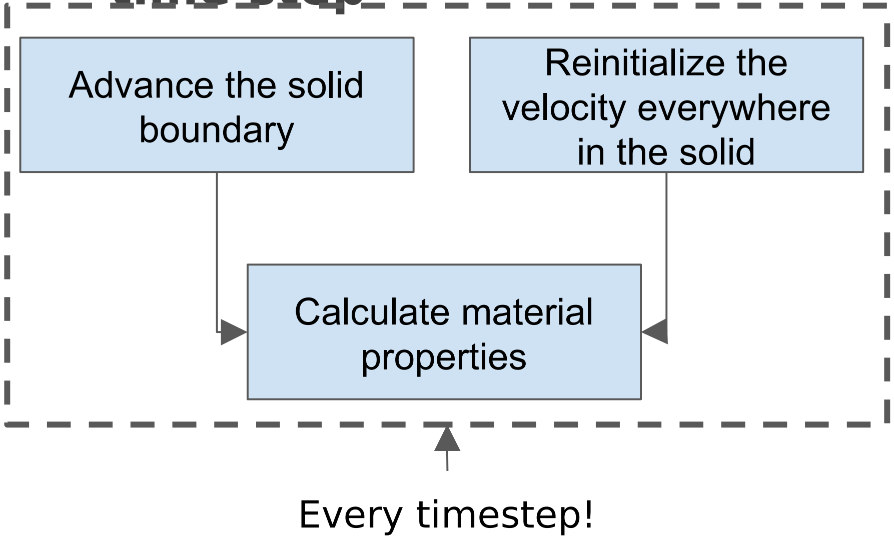

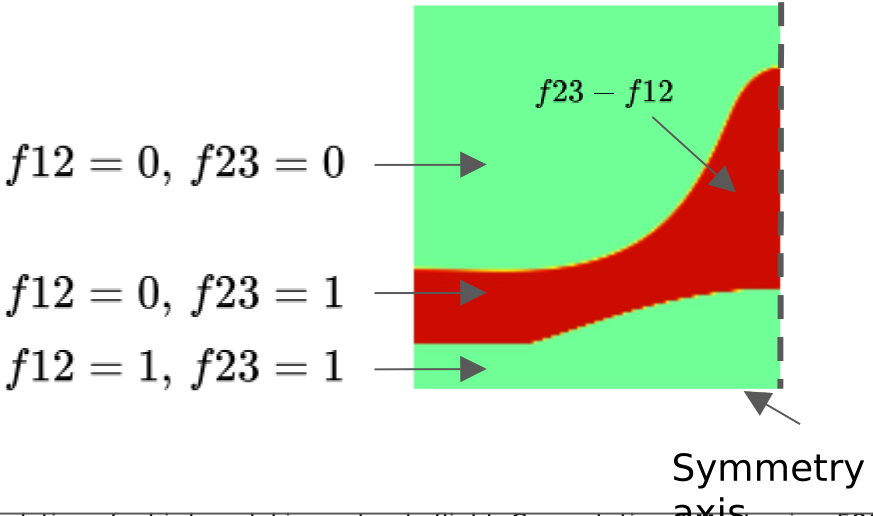

[1] Lin-Lin, Z., Hui, G., & Chui-Jie, W. (2016). Three-dimensional numerical simulation of a bird model in unsteady flight. Computational Mechanics, 58(1), 1-11.
[2] Wu, C. J., & Wang, L. (2007). Direct numerical simulation of self-propelled swimming of 3d bionic fish school. Computational Mechanics, Proceedings of ISCM.
[3] http://basilisk.fr/sandbox/popinet/movingcylinder.c

Results

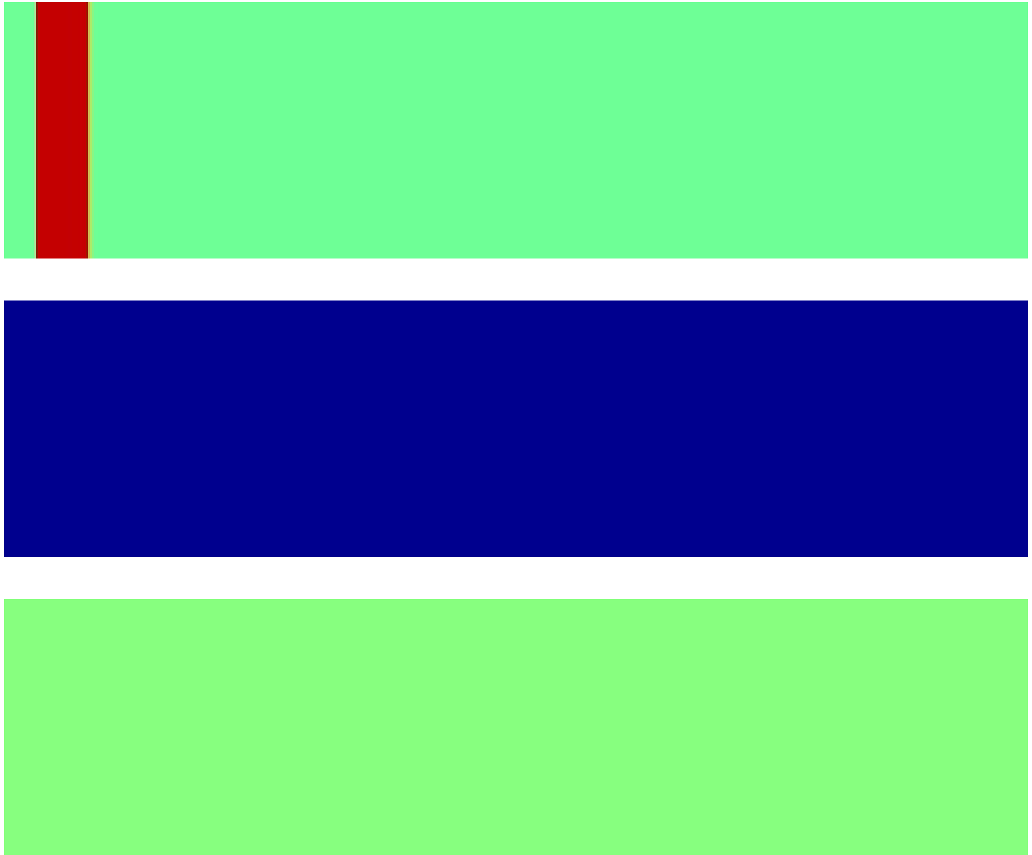

Grid Convergence

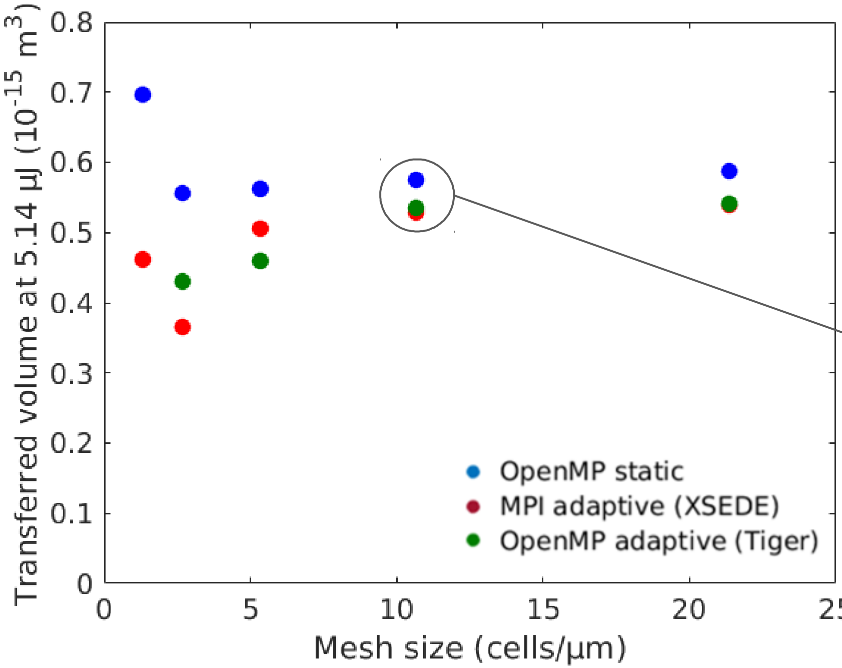

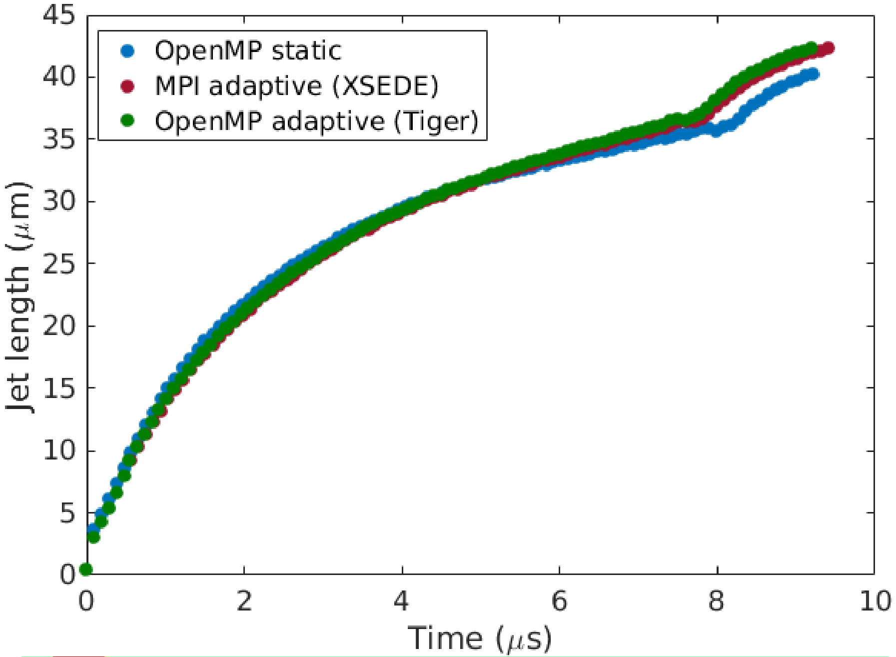

Level	7	8	9	10	11
cells/μm	1.34	2.67	5.34	10.68	21.37

Validation with Experiments

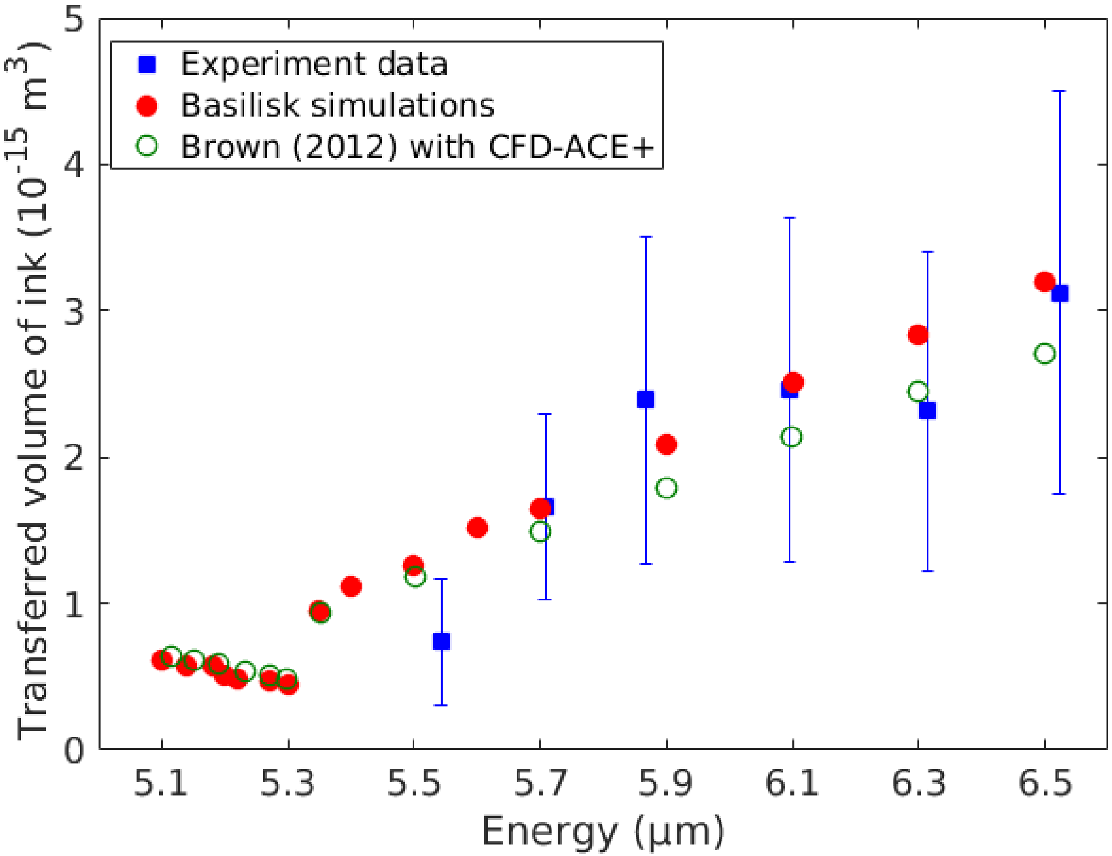

Now: Viscoelastic Models

Develop a fully adaptive Basilisk model to simulate BA-LIFT with Newtonian fluids

Determine the dimensionless parameters

Solid boundary deformation

Grid convergence with static and adaptive meshing

Validation with experiments

Transfer model

Verify the viscoelastic models in Basilisk with the literature

Modify the BA-LIFT model by introducing an extra dimensionless parameter to model viscoelasticity

A Sidetrack from BA-LIFT: Viscoelastic Simulations in Basilisk

- **Possible thanks to the model [1] implemented by Jose M. Lopez-Herrera Sanchez [2]**
  - **Log-conformation technique to overcome "the high-Weissenberg number problem"**

$$\nabla \cdot \boldsymbol{u} = 0,$$

$$\rho\left(\frac{\partial \boldsymbol{u}}{\partial t} + \boldsymbol{u}\cdot\nabla\boldsymbol{u}\right) = -\nabla p + \nabla\cdot\boldsymbol{\tau}$$

Conformation tensor!

$$\frac{\partial \mathbf{c}}{\partial t} + \mathbf{u}\cdot\nabla\mathbf{c} - (\nabla\mathbf{u}\cdot\mathbf{c} + \mathbf{c}\cdot\nabla\mathbf{u}^T) = f_s(\mathbf{c})$$

$$\boldsymbol{\tau} = \boldsymbol{\tau}_S + \boldsymbol{\tau}_P$$

$$\boldsymbol{\tau}_S = 2\eta_S \boldsymbol{D} \quad \boldsymbol{D} = (\nabla\boldsymbol{u} + \nabla\boldsymbol{u}^T)/2$$

$$\boldsymbol{\tau}_P = G_0 f_S(\mathbf{c}) \quad G_0 = \lambda_p/\eta_p$$

$$\mathrm{De} = \frac{\lambda_p}{\sqrt{\rho h^3/\gamma}} \qquad \beta = \mu_s/\mu_0$$

Oldroyd-B

$$f_s(\mathbf{c}) = \mathbf{c} - \mathbf{I}$$

FENE-P

$$f_s(\mathbf{c}) = \frac{\mathbf{c}}{1 - tr(\mathbf{c})/L^2} - \mathbf{I}$$

[1] R. Fattal and R. Kupferman. Time-dependent simulation of viscoelastic flows at high Weissenberg number using the log-conformation representation. Journal of Non-Newtonian Fluid Mechanics. 1, pp. 23–27, (2005).
[2] http://basilisk.fr/sandbox/lopez/log_conform_1.h

Verifying the Oldroyd-B model: Comparison with Clasen [1]

Clasen [1]

- 1D along the axial direction
- Finite-difference Slender jet equations

Basilisk

- 2D axially symmetric
- Log-conformation technique

Experimental image sequence

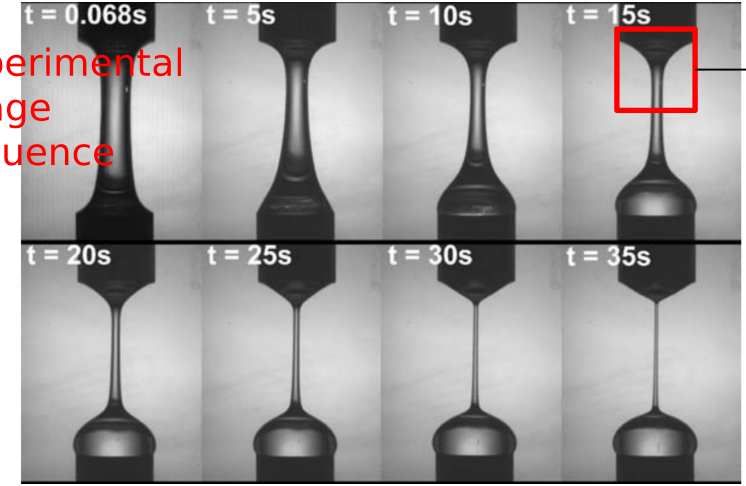

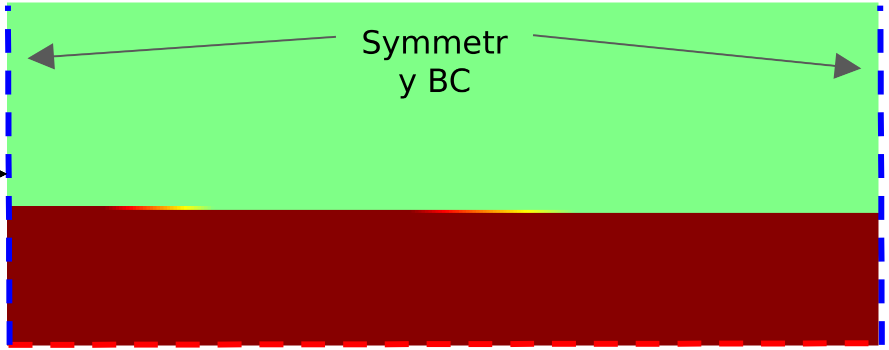

Symmetry axis

[1] Clasen, C., Eggers, J., Fontelos, M. A., Li, J., & McKinley, G. H. (2006). The beads-on-string structure of viscoelastic threads. Journal of Fluid Mechanics, 556, 283-308.

Minimum Filament Radius vs. Time

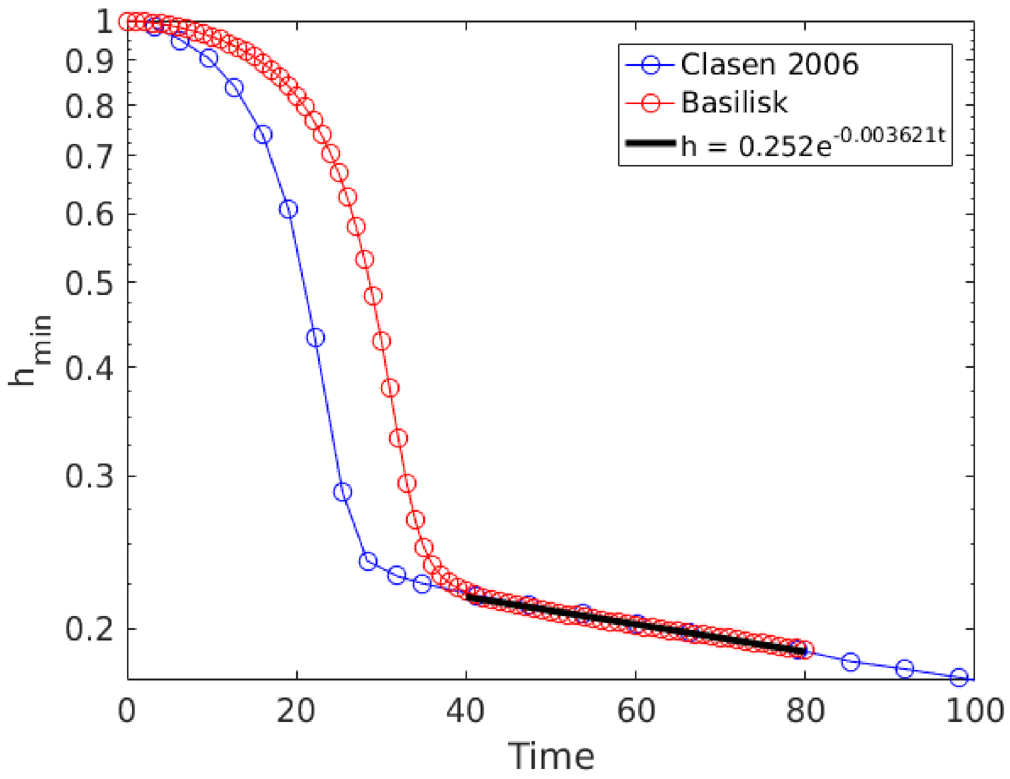

Oldroyd-B with Basilisk: Accuracy

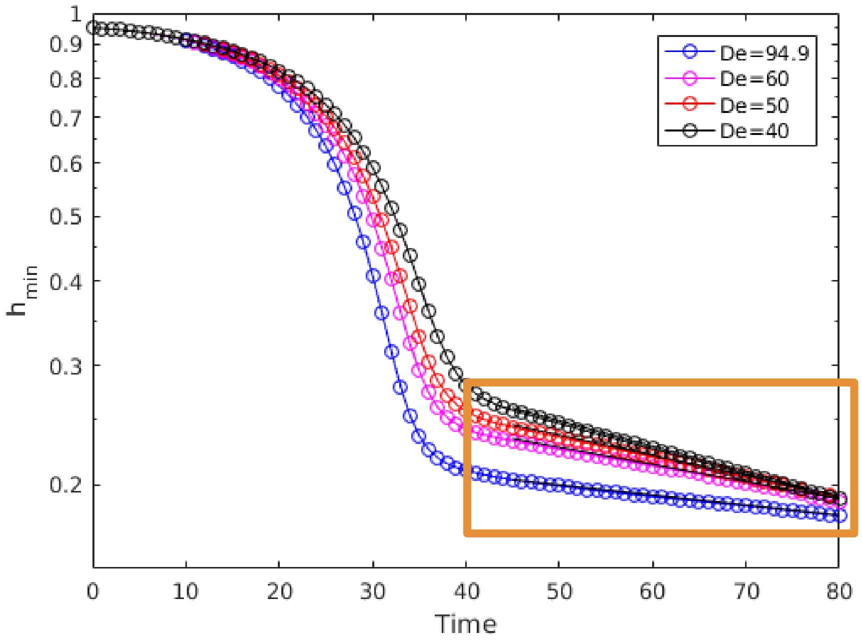

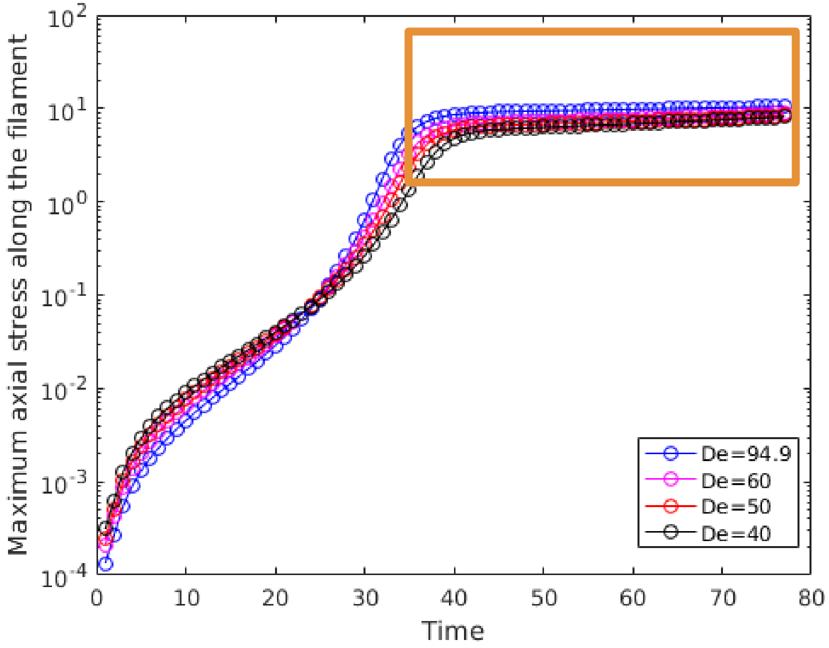

$$h(t) = h_0 \exp(-1/3\mathrm{De})$$

$$\sigma_{zz}(t) = \sigma_0 \exp(1/3\mathrm{De})$$

Oldroyd-B with Basilisk: Accuracy

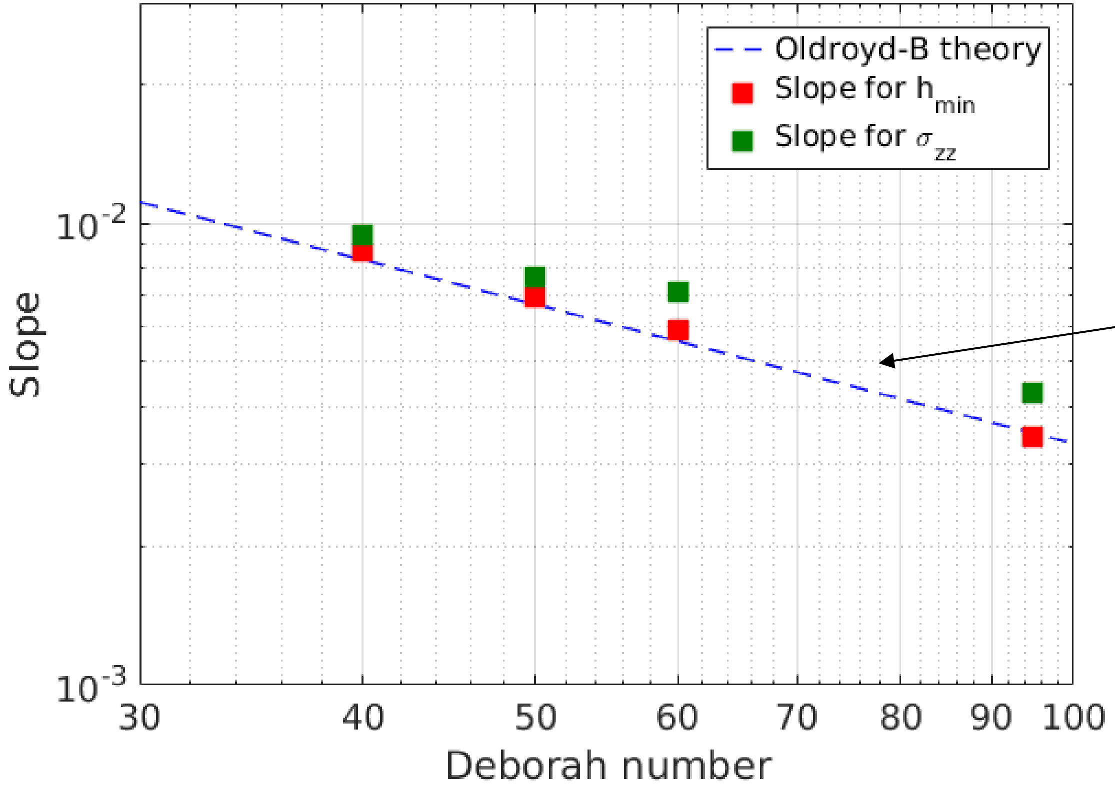

$$h(t) = h_0 \exp(-1/3\mathrm{De})$$

$$\sigma_{zz}(t) = \sigma_0 \exp(1/3\mathrm{De})$$

Slope for the axial stress should be improved!

A different strategy to solve Oldroyd-B equations?

A note on Oldroyd-B: Comparison with Experiments

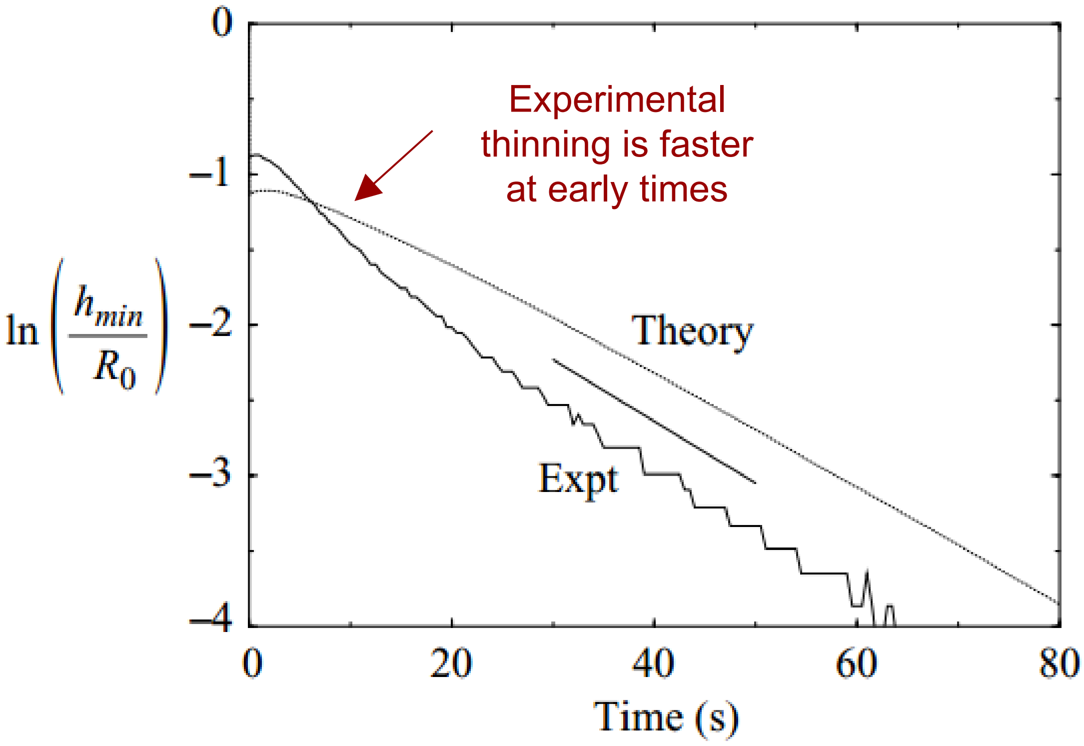

[1] Clasen, C., Eggers, J., Fontelos, M. A., Li, J., & McKinley, G. H. (2006). The beads-on-string structure of viscoelastic threads. Journal of Fluid Mechanics, 556, 283-308.

Simulating BA-LIFT with Oldroyd-B and FENE-P

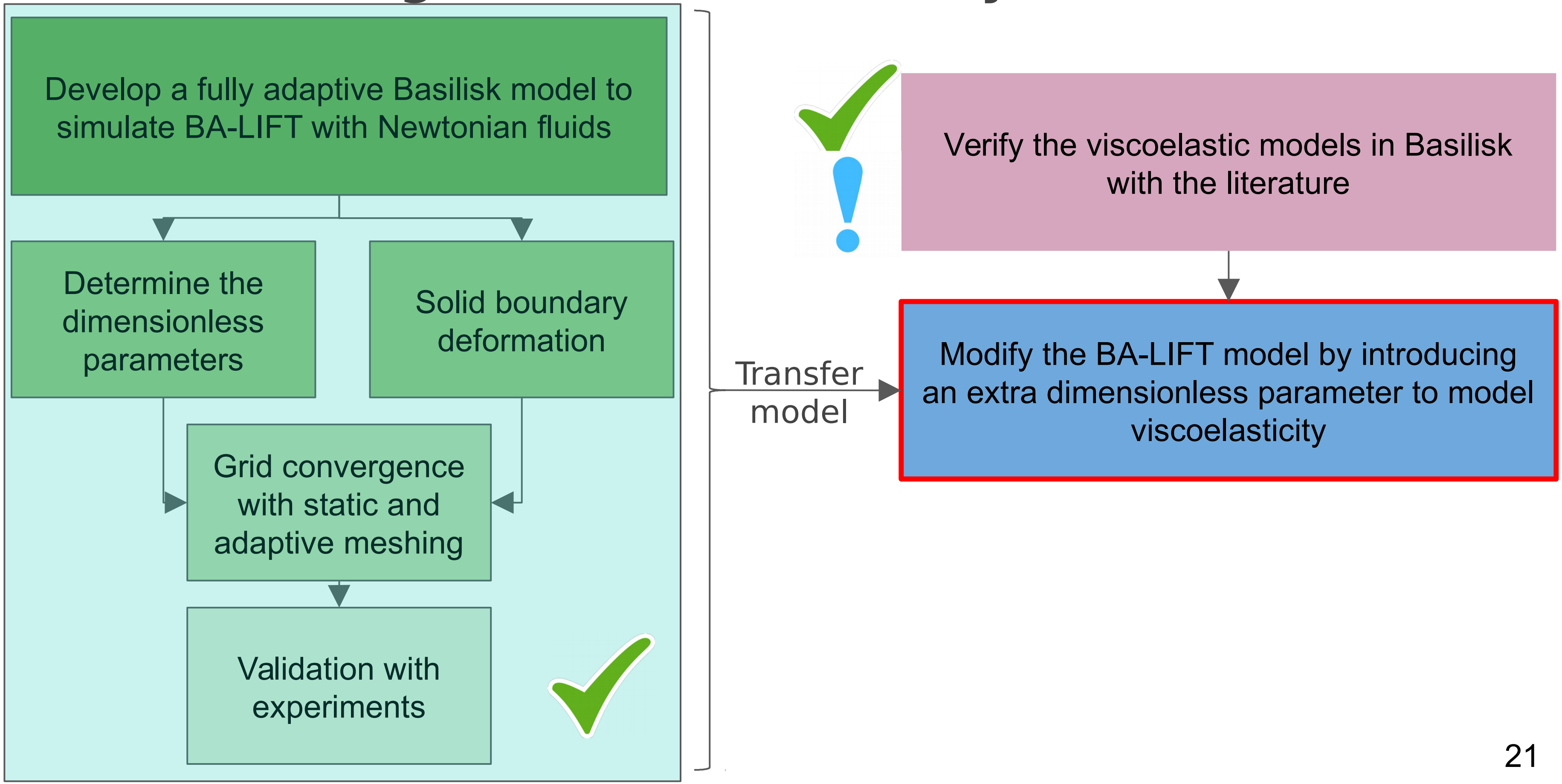

Unique Jet Features during BA-LIFT with Viscoelastic Inks

Jetting without breakup

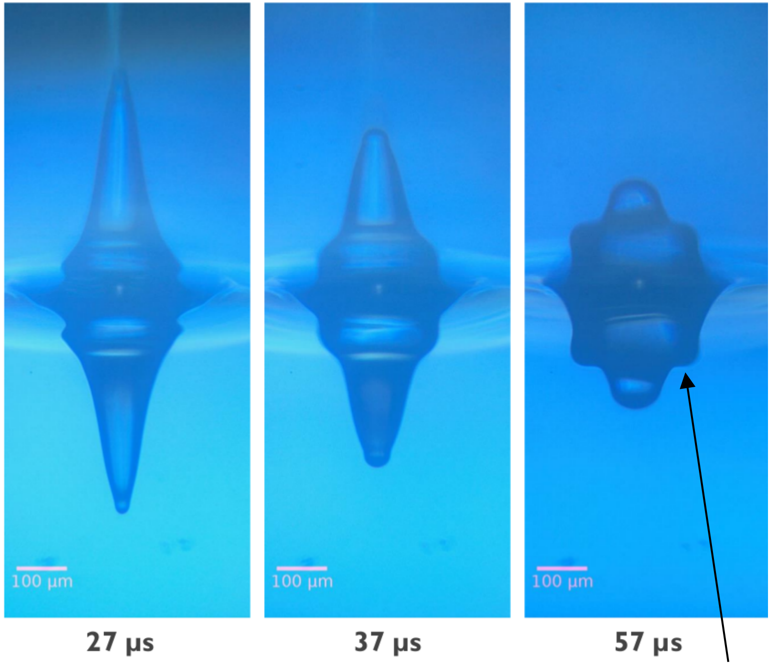

Multiple-drop formation

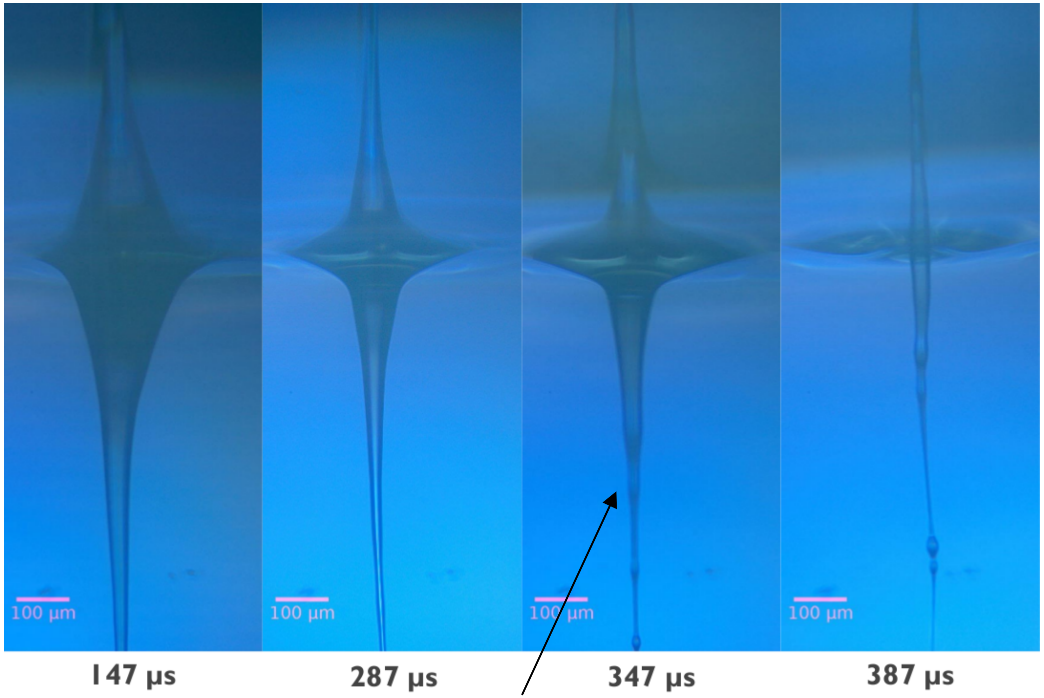

Shoulder formation

Hanging drop formation and delayed breakup

0.1 wt.% PEO in 60-40 wt.% WG

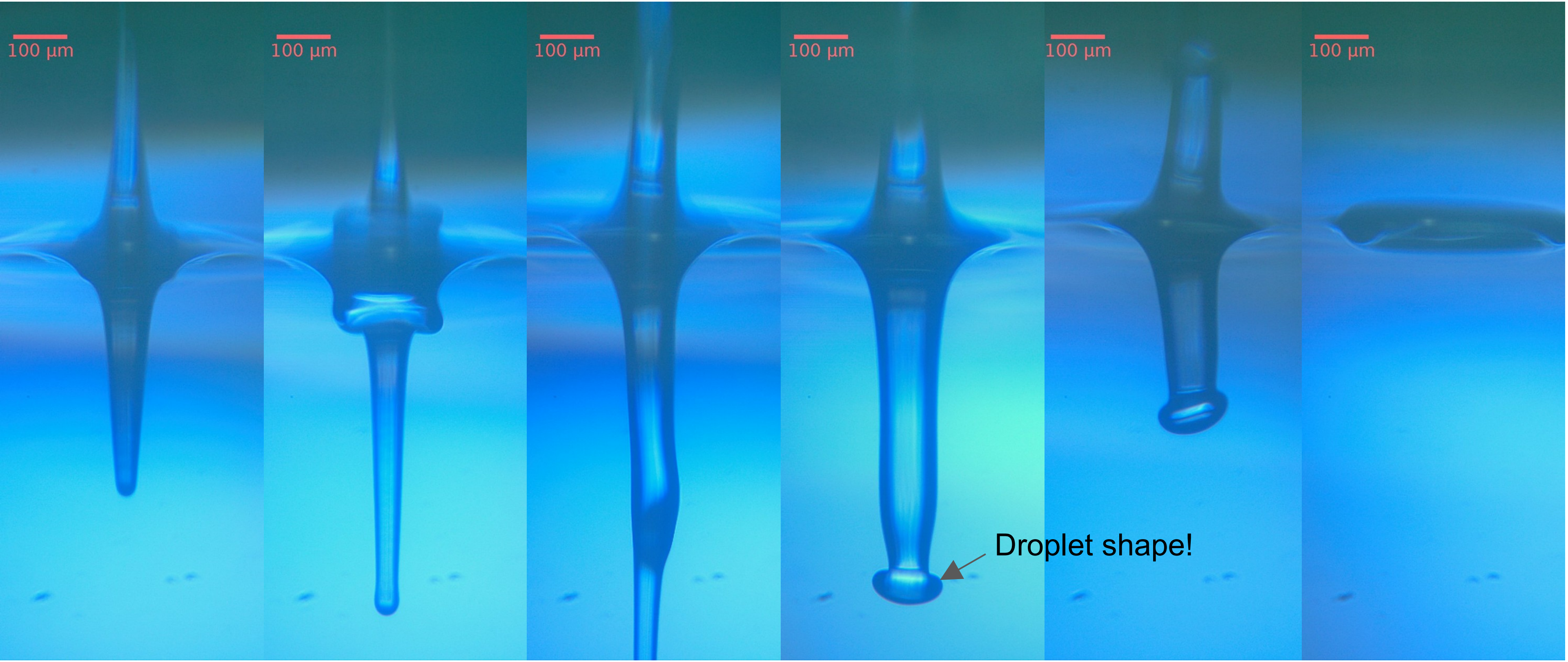

22 us | 42 us | 62 us | 292 us | 342 us | >1s

Strategy: Try to observe these features with a parameter sweep and compare with experimental parameters!

Oldroyd-B model

Can resolve with uniform mesh level 11

Infinitely stretchable polymer chains

Could not get adaptive meshing + MPI work with viscoelastic model yet!

Future Work

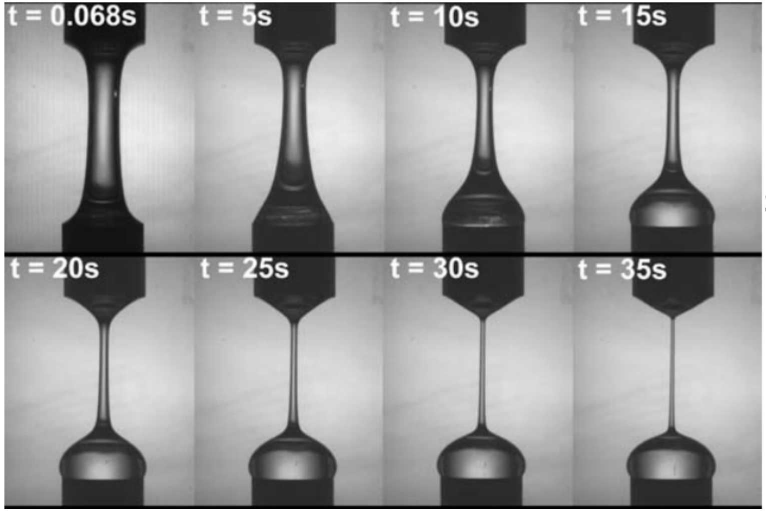

Later stages: Beads-on-a-string formation

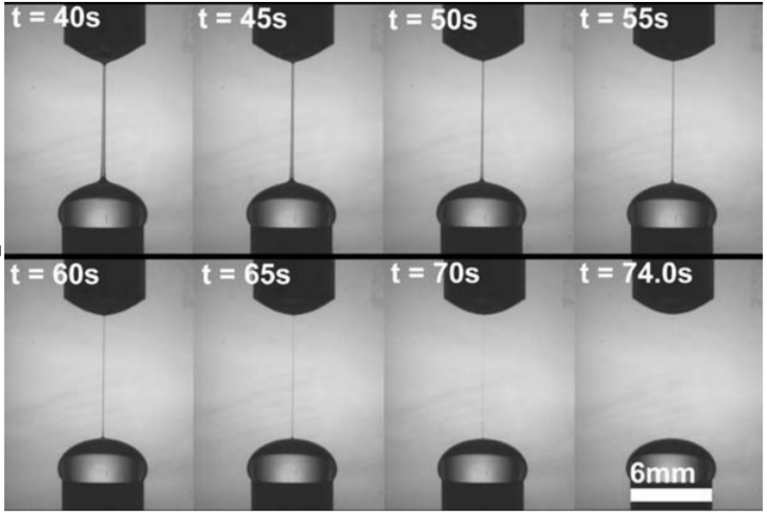

Implement refinement with filament radius

Make it work with adaptive and MPI

A model proposed in [1] to explain this sinusoidal instability!

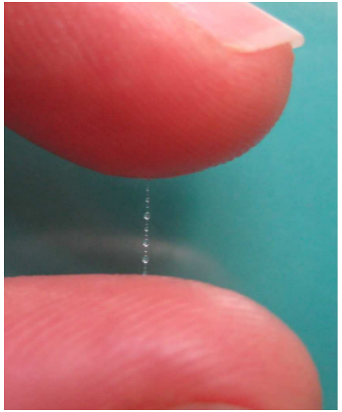

[1] Eggers, J. (2014). Instability of a polymeric thread. Physics of Fluids, 26(3), 033106.

Acknowledgements

- Members of the Arnold group

- Jose M. Lopez-Herrera Sanchez for numerous e-mail exchanges

- Prof. Jens Eggers

- Antonio Perazzo and Prof. Howard A. Stone

Future Work: We need to implement a better model! [1]

$$\rho \frac{D\mathbf{v}}{Dt} = -\nabla p + \nabla \cdot \boldsymbol{\sigma}_p + \eta_s \Delta \mathbf{v}$$

Experimental observation: Polymer concentration is very high along the thread

$$\frac{D\boldsymbol{\sigma}_p}{Dt} = (\nabla \mathbf{v})^T \cdot \boldsymbol{\sigma}_p + \boldsymbol{\sigma}_p \cdot (\nabla \mathbf{v}) - \frac{\boldsymbol{\sigma}_p}{\lambda} + nk_B T \left((\nabla \mathbf{v})^T + (\nabla \mathbf{v})\right) - k_B T \frac{Dn}{Dt}\boldsymbol{\delta} + D\Delta\boldsymbol{\sigma}_p$$

$$\frac{Dn}{Dt} = -\frac{D}{k_B T}\nabla\nabla : \boldsymbol{\sigma}_p + D\Delta n$$

n	Polymer number density
$\boldsymbol{\sigma}_p$	Polymer stress component
η_s	Solvent viscosity
λ	Relaxation time
D	Diffusivity of polymer in the solvent
$\boldsymbol{\delta}$	Unit tensor

Perturbation analysis yields a novel mechanism for an instability which grows sinusoidally and might explain the formation of beads-on-a-string structure

[1] Eggers, J. (2014). Instability of a polymeric thread. Physics of Fluids, 26(3), 033106.

Algorithm for Log-conformation Technique (as in log_conform_1.h by Lopez)

- Initialize parameters S, ψ (tensor type)
- Assign Neumann BC for S and ψ except for the axi bottom
- Evaluate A from S: $\mathbf{A} = \frac{\lambda}{\mu_p}\mathbf{S} + \mathbf{I}$
- Diagonalize A and evaluate ψ: $\psi = \log(A) = R\log(\lambda)R^T$
- Evaluate B, M and Ω
- Evaluate the RHS of (2)
- Calculate (1)
- Integrate (2)
- Recover the conformation tensor $A = e^{\psi}$
- Integrate (3) analytically
- Evaluate the stress tensor S for the next time step

1. $$\frac{\partial \psi}{\partial t} + \nabla \cdot (\psi \mathbf{u}) = 0$$

2. $$\frac{\partial \psi}{\partial t} = 2B + (\Omega \cdot \psi - \psi \cdot \Omega)$$

3. $$\frac{\partial A}{\partial t} = \frac{1}{\lambda}(I - A)$$

$$\begin{pmatrix} m_{11} & m_{12} \\ m_{21} & m_{22} \end{pmatrix} = R^{\mathrm{T}}(\nabla \mathbf{u})R \qquad B = R\begin{pmatrix} m_{11} & 0 \\ 0 & m_{22} \end{pmatrix}R^{\mathrm{T}}, \qquad \boldsymbol{\omega} = R\begin{pmatrix} 0 & \omega \\ -\omega & 0 \end{pmatrix}R^{\mathrm{T}}$$

Minimum Filament Radius vs. Time

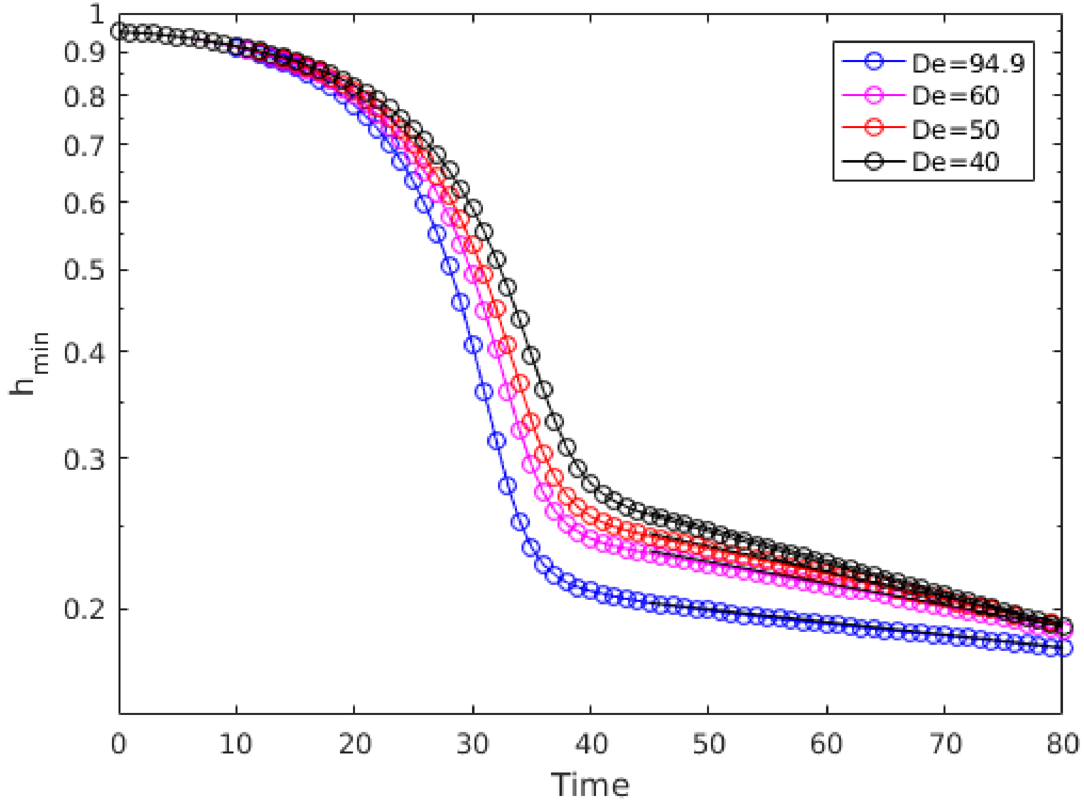

$$h(t) = h_0 \exp(-1/3\text{De}^*)$$

De	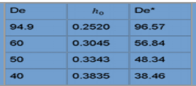	De*
94.9	0.2520	96.57
60	0.3045	56.84
50	0.3343	48.34
40	0.3835	38.46

De	h_0	De*
94.9	0.2520	96.57
60	0.3045	56.84
50	0.3343	48.34
40	0.3835	38.46

Effect of elasticity on BA-LIFT jets
Still localized pinch-off & beads-on-a-string not

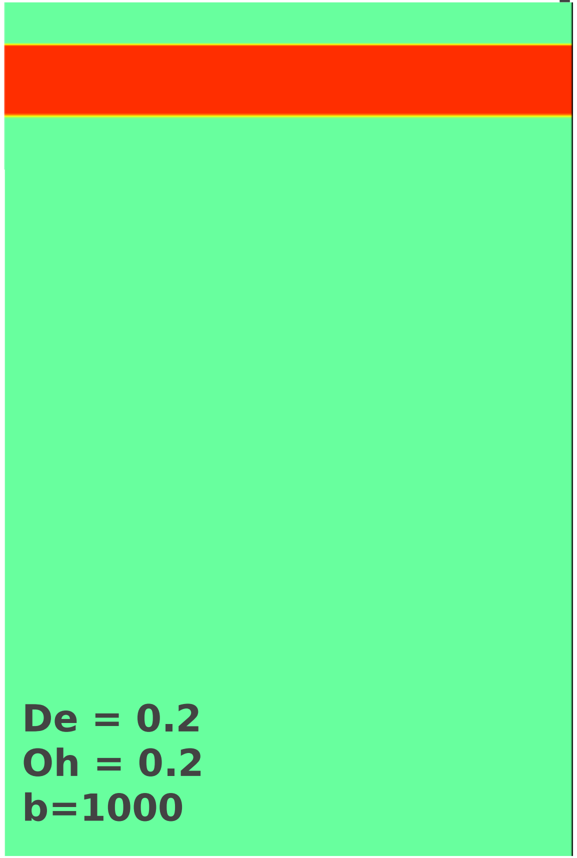

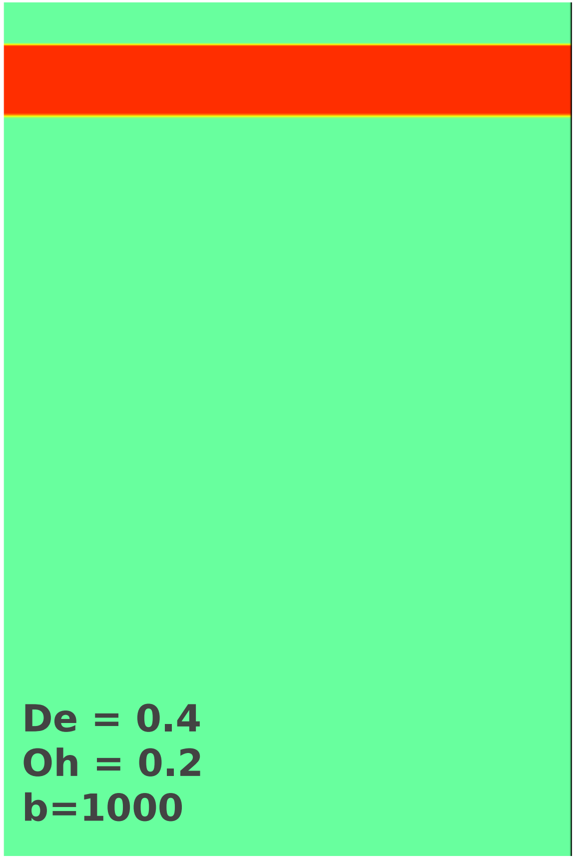

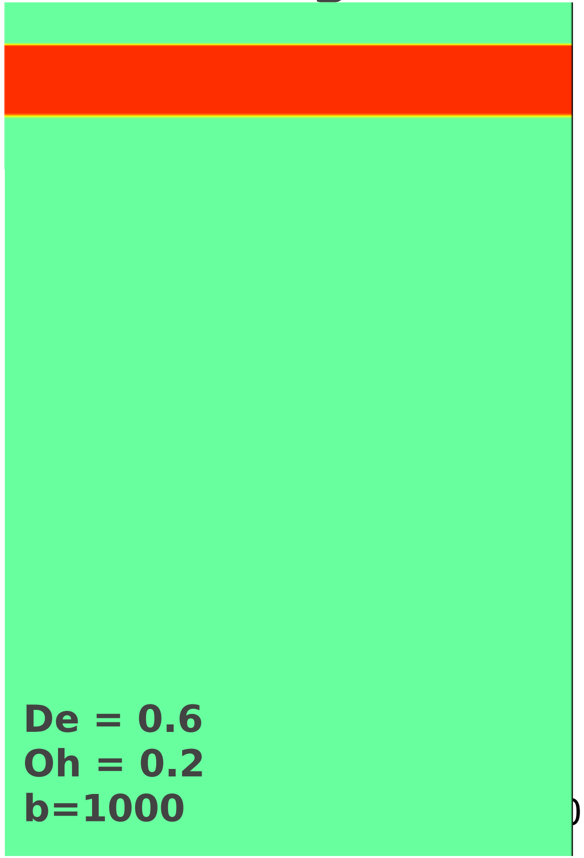

Maximum Axial Stress along the Filament vs. Time

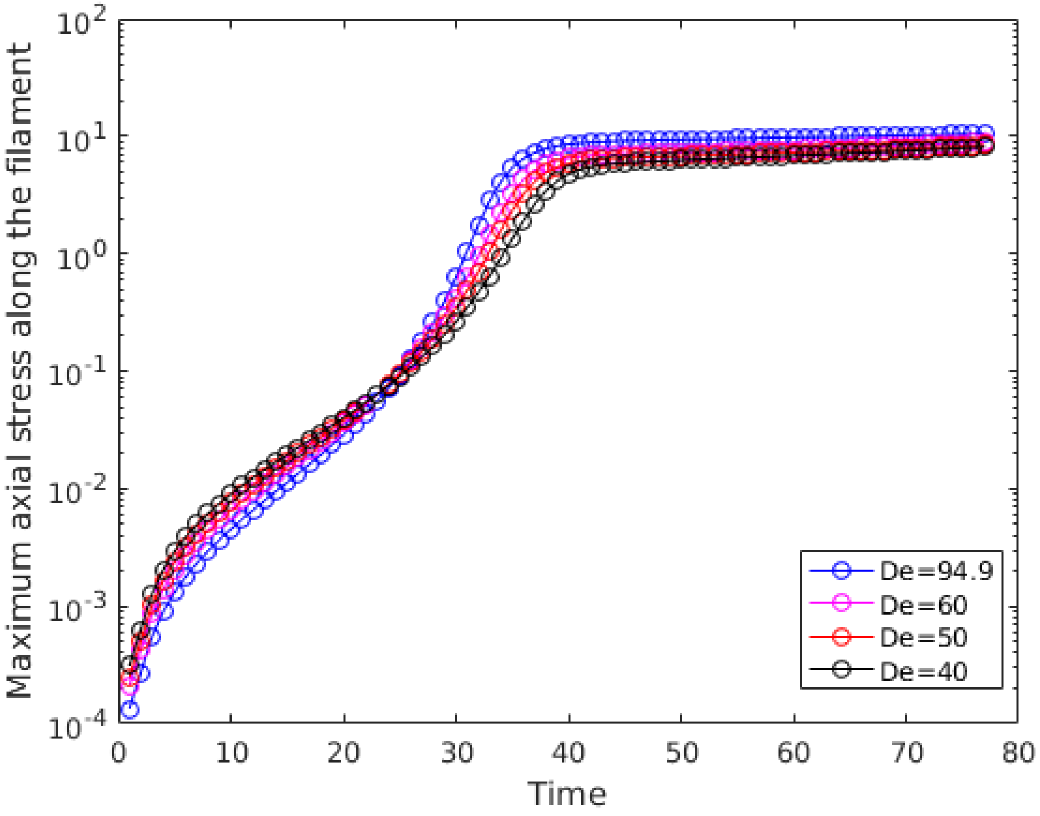

$$\sigma_{zz}(t) = \sigma_0 \exp(1/3\mathrm{De}^*)$$

$$\sigma_0 = 2/h_0$$

De			De*
94.9	0.2374	7.564	77.88
60	0.3045	5.063	47
50	0.3343	4.616	43.75
40	0.3835	3.918	35.43

De	h_0	σ_0	De*	De	h_0	σ_0	De*
94.9	0.2374	7.564	77.88	94.9	0.2374	7.564	77.88
60	0.3045	5.063	47	60	0.3045	5.063	47
50	0.3343	4.616	43.75	50	0.3343	4.616	43.75
40	0.3835	3.918	35.43	40	0.3835	3.918	35.43